

Inferred Properties of Planets in Mean-Motion Resonances are Biased by Measurement Noise

DAVID JENSEN¹ AND SARAH C. MILLHOLLAND^{2,3,4}

¹*Department of Physics, Princeton University, Princeton, NJ 08544, USA*

²*Department of Physics, Massachusetts Institute of Technology, Cambridge, MA 02139, USA*

³*MIT Kavli Institute for Astrophysics and Space Research, Massachusetts Institute of Technology, Cambridge, MA 02139, USA*

⁴*Department of Astrophysical Sciences, Princeton University, Princeton, NJ 08544, USA*

ABSTRACT

Planetary systems with mean-motion resonances (MMRs) hold special value in terms of their dynamical complexity and their capacity to constrain planet formation and migration histories. The key towards making these connections, however, is to have a reliable characterization of the resonant dynamics, especially the so-called “libration amplitude”, which qualitatively measures how deep the system is into the resonance. In this work, we identify an important complication with the interpretation of libration amplitude estimates from observational data of resonant systems. Specifically, we show that measurement noise causes inferences of the libration amplitude to be systematically biased to larger values, with noisier data yielding a larger bias. We demonstrated this through multiple approaches, including using dynamical fits of synthetic radial velocity data to explore how the the libration amplitude distribution inferred from the posterior parameter distribution varies with the degree of measurement noise. We find that even modest levels of noise still result in a slight bias. The origin of the bias stems from the topology of the resonant phase space and the fact that the available phase space volume increases non-uniformly with increasing libration amplitude. We highlight strategies for mitigating the bias through the usage of particular priors. Our results imply that many known resonant systems are likely deeper in resonance than previously appreciated.

1. INTRODUCTION

Mean-motion resonance (MMR) refers to an orbital configuration in which two bodies have orbital periods that form a ratio of small integers. These resonances were first studied in the context of the Solar System (Peale 1976), most notably the Galilean satellites around Jupiter, which form a 4:2:1 resonant chain. Most known extrasolar planets do not display resonant relationships (Fabrycky et al. 2014), although they are also not particularly rare either. Resonant chains like the famous TRAPPIST-1 system are intriguing examples (Gillon et al. 2017). Compared to planets found in transit surveys, MMRs are more common in systems discovered with radial velocities (RVs), which contain predominantly giant planets (Wright et al. 2011).

Resonant planetary systems are valuable because they provide a relic of the system’s formation history. That is, MMRs are established through convergent migration, particularly migration arising from planet-disk interac-

tions while the planets are still embedded in the proto-planetary disk (Goldreich & Tremaine 1980; Terquem & Papaloizou 2007). The current state of a resonant system can thus, in principle, provide some insight into the formation conditions and other details of the migration process (e.g. Batygin et al. 2015; Mills et al. 2016; Silburt & Rein 2017; Delisle 2017; Millholland & Laughlin 2019; Hadden & Payne 2020).

One of the most important diagnostics of a resonance is the “libration amplitude”, which is qualitatively related to the energy of the resonance and conveys the proximity of the system to “exact” resonance. Specifically, the libration amplitude reflects the range of oscillations of the planetary conjunctions around their equilibria. The libration amplitude is thought to provide constraints on how smooth or turbulent the migration was (e.g. Dempsey & Nelson 2018; Hühn et al. 2021). Resonances with very small libration amplitudes indicate very smooth and dissipative formation (Hadden & Payne 2020), whereas large libration amplitudes could be a consequence of stochastic forcing (e.g. Adams et al. 2008; Rein & Papaloizou 2009). A large libration amplitude could also indicate a history of perturbations by

another planet (e.g. Dawson et al. 2021) or overstable librations (Goldreich & Schlichting 2014; Nesvorný et al. 2022).

Given the value of the libration amplitude as a tracer of various formation processes, it is crucial to be able to obtain accurate estimates of this quantity from observations of resonant systems. Unfortunately, Millholland et al. (2018) showed that this may be in jeopardy. They found preliminary evidence (as detailed in Section 2) that the libration amplitude inferred from data of resonant systems may be systematically biased to larger values due to measurement uncertainties, in a similar way as eccentricity inferences are affected by measurement noise (e.g. Lucy & Sweeney 1971; Shen & Turner 2008; Hogg et al. 2010). Though this was suggested, it has not yet been confirmed in detail. In this paper, we use multiple approaches of confirming the bias (Sections 3 and 4) and understanding its origin (Section 5).

2. THE RESONANT LIBRATION AMPLITUDE AND BIAS FROM MEASUREMENT NOISE

One of the key measures of mean-motion resonance is the “critical angle” (also called “critical argument” or “resonant argument”). For two planets in a first-order $p + 1 : p$ MMR, there are two critical angles,

$$\begin{aligned}\phi_{12,1} &= (p + 1)\lambda_2 - p\lambda_1 - \varpi_1 \\ \phi_{12,2} &= (p + 1)\lambda_2 - p\lambda_1 - \varpi_2,\end{aligned}\quad (1)$$

where λ_1 and λ_2 are the mean longitudes of the inner and outer planets and ϖ_1 and ϖ_2 are the longitudes of pericenter. The critical angles describe the evolution of the planetary conjunctions with respect to the pericenters of the two orbits. When a system is in resonance, one or more of the critical angles undergo librations (bounded oscillations) about their equilibria. The “resonant libration amplitude” is the amplitude of these oscillations and is related to the total energy of the system, with smaller amplitudes corresponding to lower energies (Murray & Dermott 1999). Systems with zero libration amplitude are maximally damped to their resonant fixed points.

Millholland et al. (2018) first identified a possible bias of libration amplitude estimates as part of their detailed characterization of the GJ 876 system. GJ 876 is a nearby M4V dwarf hosting four known planets, the outer three of which are locked in a 4:2:1 Laplace resonance (Marcy et al. 2001; Laughlin et al. 2005; Rivera et al. 2005, 2010; Nelson et al. 2016; Millholland et al. 2018). The 2:1 MMR of planets c and b (the second and third planets from the star with $P_c \sim 30$ days and $P_b \sim 61$ days) was the first resonance discovered in an explan-

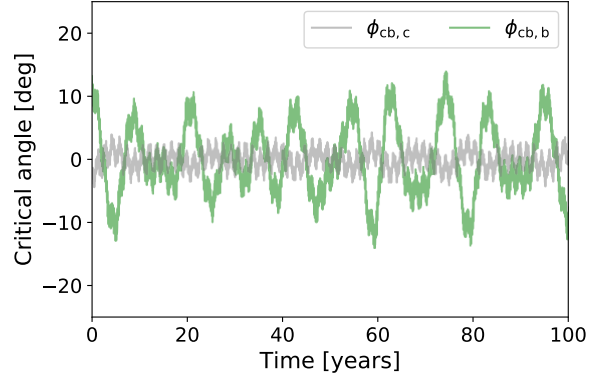


Figure 1. Evolution of two critical resonant angles resulting from a numerical integration of the GJ 876 system. The two angles correspond to the 2:1 MMR between planets c and b.

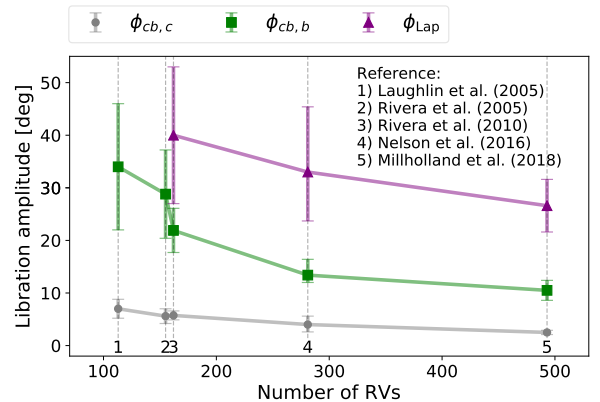


Figure 2. Published estimates of the libration amplitudes of three critical resonant angles ($\phi_{cb,c}$, $\phi_{cb,b}$, ϕ_{Lap}) in the GJ 876 system, plotted as a function of the number of radial velocity measurements used in the analysis. These results are taken from Laughlin et al. (2005), Rivera et al. (2005), Rivera et al. (2010), Nelson et al. (2016), and Millholland et al. (2018). Measurements from ELODIE, CORALIE, or Lick Observatory are not included in the number of RVs. (Figure adapted from Millholland et al. 2018.)

etary system. This MMR has two critical angles,

$$\begin{aligned}\phi_{cb,c} &= 2\lambda_b - \lambda_c - \varpi_c \\ \phi_{cb,b} &= 2\lambda_b - \lambda_c - \varpi_b.\end{aligned}\quad (2)$$

In Figure 1, we plot the evolution of $\phi_{cb,c}$ and $\phi_{cb,b}$ for a 100 year N -body integration of the GJ 876 system using the best-fit parameters identified in Millholland et al. (2018) as initial conditions. We use the REBOUND gravitational dynamics software package (Rein & Liu 2012) with the “WHFast” Wisdom-Holman symplectic integrator (Wisdom & Holman 1991; Rein 2015). The angles undergo low amplitude librations around 0° . There are additional angles analogous to $\phi_{cb,c}$ and $\phi_{cb,b}$

for the 2:1 resonance of planets b and e (the third and fourth planets from the star). Beyond the individual two-body critical angles, the three-body 4:2:1 Laplace resonance of planets c, b, and e is further defined by the libration of the critical angle,

$$\phi_{\text{Lap}} = \lambda_c - 3\lambda_b + 2\lambda_e. \quad (3)$$

Given the long history of explorations of GJ 876 by different research teams, one can explore how the libration amplitude estimates have changed with the size of the RV datasets. Millholland et al. (2018) showed that the reported libration amplitudes decreased monotonically with each successive characterization of the system. Figure 2 shows the amplitude estimates of $\phi_{cb,c}$, $\phi_{cb,c}$, and ϕ_{Lap} from different publications as a function of the number of RV measurements used in the analyses. Each study deemed the system to be deeper in resonance than all previous studies. Since a larger dataset corresponds to a higher signal-to-noise ratio, this finding may indicate that measurement noise causes resonant systems to appear to have larger libration amplitudes than they actually do. The true state of the system may be even lower energy than the latest measurements indicate.

The above hypothesis – that measurement noise biases libration amplitude estimates – needs to be confirmed with further analyses. One reason for this is that the different publications referenced in Figure 1 used a variety of analysis techniques, including both Bayesian and non-Bayesian methods, so the comparisons between them cannot be directly mapped to differences in signal-to-noise ratios. It would be more instructive to use the same analysis methods on the same dataset and systematically vary either the signal-to-noise ratio or the size of the dataset. Moreover, this would allow us to not only confirm the existence of the bias but also understand its origin. We will explore these concepts in the following sections.

Before proceeding, however, we must clarify exactly what we mean with our usage of the term “bias”. In frequentist statistics, an estimator $\hat{\theta}$ of a parameter θ is “unbiased” if $\text{Bias}(\theta) = \text{E}(\hat{\theta}) - \theta = 0$, or in other words, if the expected value of the estimator is equal to the true value of the parameter being estimated. The concept of bias is ill-defined in Bayesian statistics, in part because the parameter itself is not considered to be fixed, but rather it is a random variable whose probability distribution we wish to estimate with the inclusion of the prior probability. In this paper we use the term “bias” loosely in order to refer to the phenomenon in which progressively larger measurement noise leads the posterior parameter distribution to be increasingly weighted towards larger (or smaller) values. The libration ampli-

tude “bias” discussed herein is very analogous to that which plagues the inference of orbital eccentricities (e.g. Lucy & Sweeney 1971; Shen & Turner 2008; Hogg et al. 2010), although an important difference is that the eccentricity is generally a parameter of the orbit model, whereas the libration amplitude is not.

3. EXPLORING THE BIAS

Although the hypothesized libration amplitude bias was first identified in the GJ 876 system, it is useful to use a simpler resonant system to explore the bias further. For this purpose, we consider the HD 128311 system, which contains two eccentric gas giant planets in a 2:1 MMR (Butler et al. 2003; Vogt et al. 2005; McArthur et al. 2014; Rein 2015). The system was most recently studied by Rein (2015), who performed a dynamical fit and determined the system to be locked in resonance with a libration amplitude of $\sim 37^\circ$. Some of the relevant best-fit system parameters from Rein (2015) are provided in Table 1. In this section, we use Rein (2015)’s posterior distributions (H. Rein, private communication) to explore the effects of measurement noise on estimates of the libration amplitude.

In general, lower signal-to-noise data results in broader posterior distributions. Accordingly, we can impose an artificial broadening of the posterior distribution as a means of simulating the effects of added measurement noise without ever touching the raw data. (Later in Section 4, we will work directly with the data.) To perform the simulated broadening, we will first demonstrate that the posterior distribution can be well-described by a multivariate Gaussian distribution.

We parameterize the posterior distribution as

$$\mathbf{X}_{\text{post}} = (\log_{10} M_{p1} \sin i, P_1, \sqrt{e_1} \cos \omega_1, \sqrt{e_1} \sin \omega_1, M_1, \log_{10} M_{p2} \sin i, P_2, \sqrt{e_2} \cos \omega_2, \sqrt{e_2} \sin \omega_2, M_2, \cos i). \quad (4)$$

Next, we calculate the mean vector $\boldsymbol{\mu}_{\text{post}}$ and covariance matrix $\boldsymbol{\Sigma}_{\text{post}}$ of \mathbf{X}_{post} such that the distribution can be closely approximated by a simulated distribution drawn according to the multivariate Gaussian,

$$\mathbf{X}_{\text{sim}} \sim \mathcal{N}(\boldsymbol{\mu}_{\text{post}}, \boldsymbol{\Sigma}_{\text{post}}). \quad (5)$$

We use visual inspection of corner plots of the true distribution and a simulated distribution with an equal sample size to verify that the distributions are similar. An example of one sub-plot of this broader corner plot is shown in the left panel of Figure 3.

To approximate the broadening of the posterior distribution that would result from noisier data, we simply

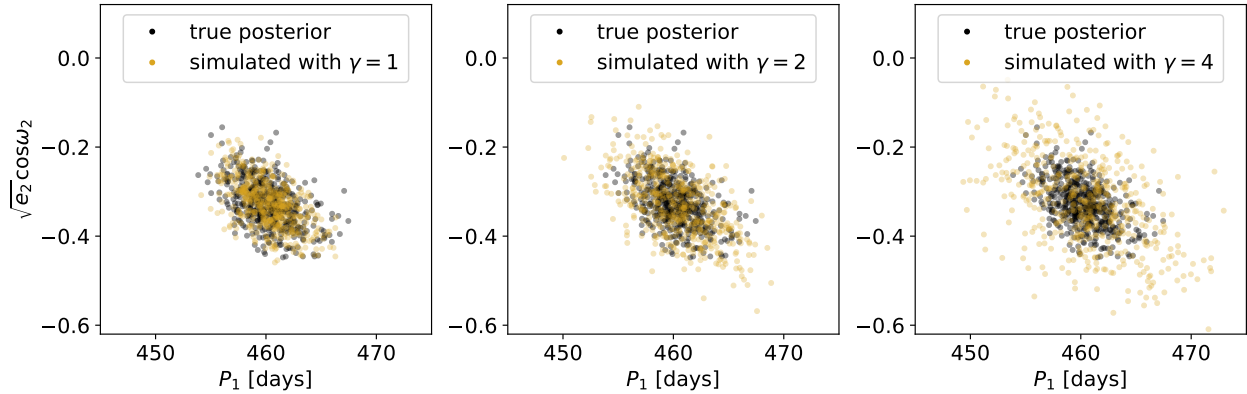


Figure 3. One example subplot ($\sqrt{e_2} \cos \omega_2$ vs. P_1) of the full corner plot of the posterior distribution, with the three panels indicating three versions of the simulated distribution with different broadening factors γ . The black (yellow) points correspond to data from the true (simulated) distributions. The simulated distribution in the left panel ($\gamma = 1$, no broadening) agrees well with the true distribution.

Table 1. Best-fit parameters of the HD 128311 system from the dynamical fit by Rein (2015).

Parameter	Value and 2σ confidence interval
Epoch	2450983.83 (fixed)
M_\star	$0.828 M_\odot$
i	$63.8^\circ_{-35.9^\circ}^{+23.7^\circ}$
Planet 1	
$M_{p1} \sin i$	$1.83_{-0.18}^{+0.15} M_{\text{Jup}}$
P_1	$460.1_{-3.6}^{+4.2}$ days
e_1	$0.30_{-0.04}^{+0.03}$
ω_1	$-76.2^\circ_{-9.2^\circ}^{+6.4^\circ}$
M_1	$259.2^\circ_{-12.6^\circ}^{+11.9^\circ}$
Planet 2	
$M_{p2} \sin i$	$3.20_{-0.08}^{+0.08} M_{\text{Jup}}$
P_2	$910.7_{-6.0}^{+7.6}$ days
e_2	$0.12_{-0.06}^{+0.08}$
ω_2	$-19.7^\circ_{-12.0^\circ}^{+23.2^\circ}$
M_2	$184.2^\circ_{-10.7^\circ}^{+20.0^\circ}$

scale the covariance matrix by a constant factor, $\gamma > 1$, such that the simulated distribution is now given by

$$\mathbf{X}_{\text{sim}} \sim \mathcal{N}(\boldsymbol{\mu}_{\text{post}}, \gamma \boldsymbol{\Sigma}_{\text{post}}). \quad (6)$$

We explore γ values ranging from 1 through 8. Examples of broadened distributions are shown in the middle and right panels of Figure 3.

We now calculate the distributions of libration amplitudes resulting from both the true and simulated posterior distributions. For each posterior sample, we use the system parameters as initial conditions and run a 1,000-year N -body integration using the

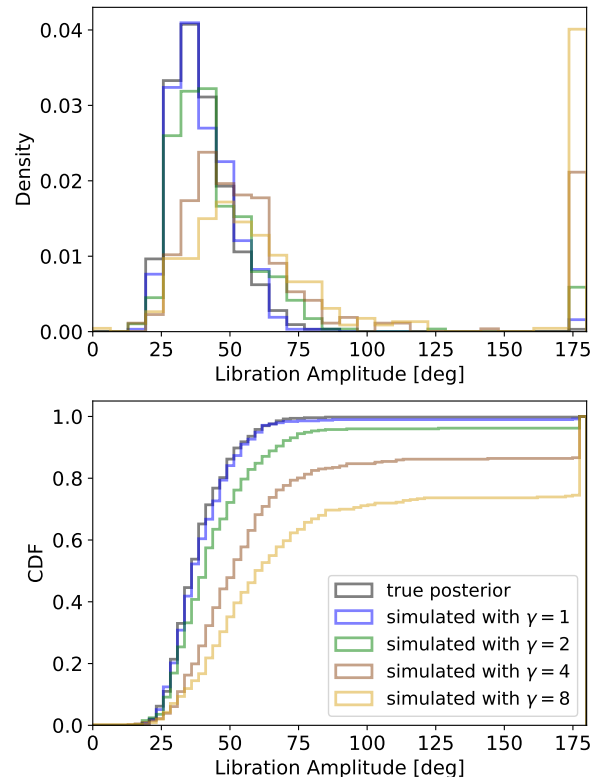


Figure 4. Libration amplitude distributions for the critical angle $\phi_1 = 2\lambda_2 - \lambda_1 - \varpi_1$ in the HD 128311 system. The result corresponding to the true posterior distribution from Rein (2015) is shown in gray. Additionally, we show the results from four simulated posterior distributions with broadening factors, γ , indicated in the legend. The top and bottom panels correspond to normalized histograms and cumulative histograms, respectively.

REBOUND gravitational dynamics software package (Rein & Liu 2012) with the “WHFast” Wisdom-Holman symplectic integrator (Wisdom & Holman 1991; Rein 2015). We calculate the critical angle $\phi_1 = 2\lambda_2 - \lambda_1 - \varpi_1$ and numerically estimate its amplitude using $A_{\text{lib}} = 0.5(\max \phi_1 - \min \phi_1)$.¹

The resulting distributions of libration amplitudes are shown in Figure 4. Here we observe, first, that the distribution resulting from the simulated posterior with $\gamma = 1$ (no broadening) closely resembles that of the true posterior, which provides further confirmation that the multivariate Gaussian approximation is appropriate. Moreover, we observe that the distributions corresponding to the simulated posteriors with $\gamma > 1$ are shifted to progressively larger libration amplitudes as the broadening factor increases. This result offers support of our primary hypothesis. Namely, the libration amplitude distribution does indeed appear to be systematically biased high as a result of noisier data, when simulated in terms of broader posterior distributions.

4. SYNTHETIC DATA EXPERIMENTS

While the previous exploration of simulated posterior distributions was supportive of our hypothesis, a more thorough examination of the hypothesis would involve systematically varying the signal-to-noise of the data. In this section, we perform dynamical fits to synthetic RV data with various levels of added noise and compare the resulting libration amplitude distributions.

We use the general parameters of the HD 128311 system. Specifically, we examine the true posterior distribution and extract the parameters of the single sample that we determined to have the lowest libration amplitude, which turns out to be $\sim 20^\circ$. We use the lowest libration amplitude configuration because we want to explore progressively larger amounts of measurement noise and see how the libration amplitude distribution shifts. We use REBOUND with the IAS15 integrator (Rein & Spiegel 2015) to generate the synthetic RV measurements with 200 data points randomly spaced over a period of 15 years. We add Gaussian noise with varying standard deviations, σ_{noise} .

Next, we employ the affine-invariant ensemble sampler `emcee` (Goodman & Weare 2010; Foreman-Mackey et al. 2013) to estimate the posterior distributions of the parameters consistent with the synthetic data. For sim-

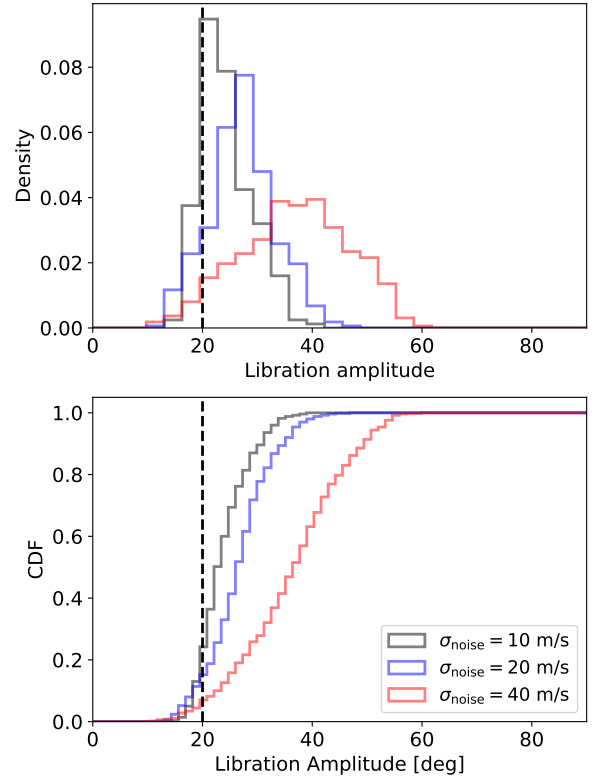


Figure 5. Libration amplitude distributions for the critical angle $\phi_1 = 2\lambda_2 - \lambda_1 - \varpi_1$ in a synthetic system closely resembling HD 128311. These results correspond to the posterior distributions resulting from the fits to the synthetic radial velocity data with varying levels of Gaussian noise with standard deviation, σ_{noise} . The top and bottom panels correspond to normalized histograms and cumulative histograms, respectively. The dashed black line corresponds to the “true” libration amplitude of the synthetic system.

plicity, we assume uninformative priors for all parameters. We use 50 walkers and sample the parameters in the same coordinate system as indicated in equation 4. We run the integration for 750 iterations and check for convergence by visual inspection of the log-probability. Finally, we take a random subset of 500 posterior samples from the chains (post burn-in) and use the procedure described in the previous section to calculate the corresponding libration amplitude distributions.

The resulting libration amplitude distributions are shown in Figure 5. Similar to Figure 4, the distributions are shifted to larger libration amplitudes as σ_{noise} increases. Moreover, even the distribution corresponding to the lowest level of noise is still systematically shifted to larger values than 20° , which is the true libration amplitude of the synthetic system. This experiment thus offers a strong confirmation of our hypothesis. That is, any amount of measurement noise will tend to systemat-

¹ We note that calculating A_{lib} from the osculating orbital elements in this manner may be another source of overestimation. This is because the osculating elements are affected by high-frequency variations at the synodic period, thus creating a non-zero minimum A_{lib} . This is probably only relevant in systems with very massive planets and tightly spaced MMRs.

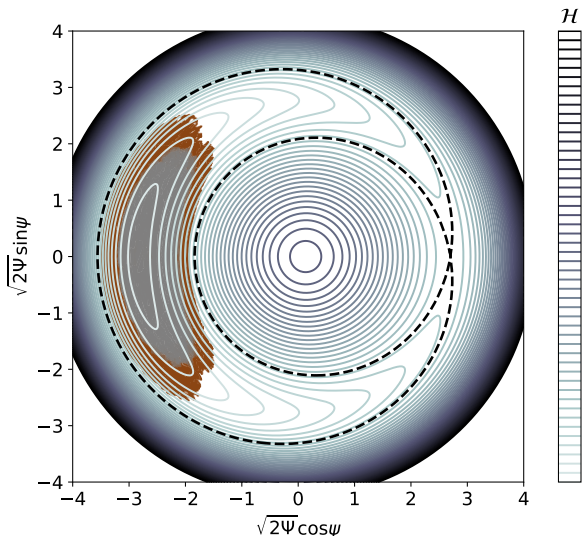


Figure 6. Phase space portrait of the approximate first-order resonant motion of HD 128311. The action-angle variables are complicated functions of the planetary orbital elements, but roughly speaking, Ψ is proportional to $\sim e^2$, and ψ is a combination of the critical angles. The level curves correspond to energy levels of the integrable one-degree-of-freedom Hamiltonian from [Batygin & Morbidelli \(2013\)](#). The dashed line indicates the separatrix, which encloses the crescent-moon-shaped resonant domain. The gray and brown regions indicate several trajectories derived from integrations of the system with parameters drawn from the true posterior distribution (gray) and the simulated distribution with $\gamma = 2$ (brown).

ically bias the libration amplitude distribution inferred from the posterior distribution, and the degree of the bias increases with the measurement noise.

5. DISCUSSION

5.1. Origin of the bias

The last two sections confirmed that the bias is indeed real. However, we haven't yet discussed its physical origin. The bias is likely caused by the fact that the available phase space volume increases non-uniformly with increasing libration amplitude. That is, if the dynamics are expressed in terms of an integrable one-degree-of-freedom approximation using Hamiltonian perturbation theory (e.g. [Henrard & Lemaître 1983](#); [Batygin & Morbidelli 2013](#); [Nesvorný & Vokrouhlický 2016](#)), then the resonant trajectories in phase space are those that are librating inside a finite resonant domain. Only a subset of this domain is available for libration amplitudes below a certain threshold. If we denote $V(A_{\text{lib}})$ as the total phase space volume occupied by resonant trajectories with libration amplitudes $\leq A_{\text{lib}}$, then dV/dA_{lib} is a positive and increasing function of A_{lib} . Thus, when the posterior distribution of system parameters is

broader due to the effects of noise, a uniform sampling of the available resonant phase space will be increasingly skewed to larger libration amplitudes.

Figure 6 demonstrates a schematic representation of this. It shows a phase space portrait of the first-order resonant Hamiltonian derived by [Batygin & Morbidelli \(2013\)](#) and applied to the parameters of the HD 128311 system. We superimpose trajectories resulting from N -body integrations of posterior samples, both from the true posterior distribution and the simulated posterior distribution with $\gamma = 2$ (Section 3). This illustration indicates that the trajectories of initial system parameters from the broadened posterior extend to a larger region of the resonant domain (and a correspondingly larger range of libration amplitudes) than the trajectories resulting from the true posterior.

Given a set of initial orbital elements, a single trajectory would ideally fall upon a single level curve. There are several reasons why the gray and brown regions are blurred out and do not follow the topology exactly. First, the analytic approximation assumes small eccentricities, but the eccentricities of the HD 128311 system ($e_1 \sim 0.3$, $e_2 \sim 0.12$) are moderate. Second, we are plotting multiple trajectories with different initial conditions, each associated with different libration amplitudes. Finally, the topology of the phase space (as indicated by the level curves) is conserved in time but varies with respect to different sets of initial system parameters. Thus, the level curves in Figure 6 can only be thought of as an average representation of the system parameters. Despite these caveats, this schematic illustration helps provide a geometric understanding of how broader posterior distributions of system parameters translate into broader available volumes in the resonant phase space and larger libration amplitudes.

5.2. Potential remedies

There are some potential strategies for remedying the bias. One approach would be to set a prior on A_{lib} to counteract the effect of the bias. The key is to realize that the bias itself is a result of the particular choice of priors. When using the uninformative priors conventionally adopted in RV models, we found in Section 4 that the marginalized posterior distributions of libration amplitudes are weighted to progressively larger values as a function of increasing measurement noise. The prior on A_{lib} is implicit in the conventional framework, but it can still be modified.

For example, when computing the posterior of a proposed MCMC sample, we can include a Gaussian-like penalty term in the prior, such that the prior on A_{lib} becomes the product of the conventional implicit prior

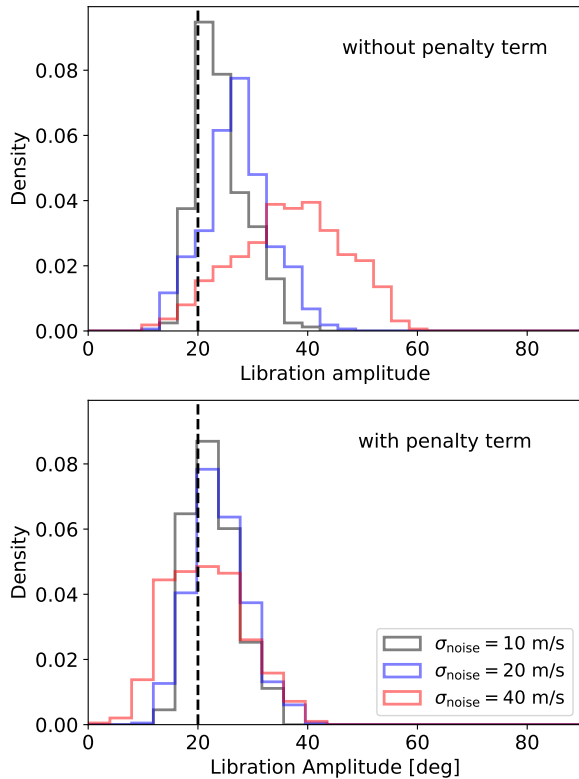


Figure 7. Libration amplitude distributions for the critical angle $\phi_1 = 2\lambda_2 - \lambda_1 - \varpi_1$ in a synthetic system closely resembling HD 128311. The top panel is a duplicate of the Figure 5 top panel for convenience. The bottom panel corresponds to the posterior distributions resulting from the MCMC sampling with a Gaussian-like penalty term included in the prior. The dashed black line corresponds to the “true” libration amplitude of the synthetic system. The medians of the $\sigma_{\text{noise}} = 10$ m/s, 20 m/s, and 40 m/s distributions are 23° , 27° , and 37° for the top panel and 22° , 23° , and 21° for the bottom panel.

and the penalty term. We test this approach by repeating our synthetic data experiments from Section 4, everything being equal except with the inclusion of the penalty term, $\exp[-A_{\text{lib}}^2/(2\sigma^2)]$, which is multiplied by the usual uninformative prior. In order to calculate A_{lib} for each proposed sample, we perform an additional “WHFast” integration with a timestep equal to 40 days, approximately 8.7% of P_1 ,² and a duration of 350 years. Performing this extra integration increases the computation time of the posterior by a factor of ~ 3 . As for the σ in the penalty term, we find through trial and error that $\sigma \approx 0.2$ (when A_{lib} is in radians) is an appropriate

² We note that this timestep is larger than what is generally recommended (Wisdom 2015). We adopted it for computational speed and verified that the resulting A_{lib} calculations are not significantly affected.

value, in the sense that it yields the desired effect on the libration amplitude distribution, as we will next show.

Figure 7 shows the resulting libration amplitude distributions when the penalty term is used. Compared to the previous case, the distributions agree much better with the true libration amplitude of the synthetic system. The distributions are broadened with increasing σ_{noise} , but they do not have the strong systematic shifts seen earlier. Accordingly, this approach is a reasonable “quick fix” to approximately counteract the bias. We caution that the optimal value of σ in the penalty term can depend on the system at hand, so in terms of an application to observed systems, one should explore a range of different σ values and examine the resulting sensitivity of the inferred system parameters to the prior.

A more formal approach to address the bias would be to construct the RV model with specific assumptions about the libration amplitude. For instance, Hadden & Payne (2020) developed an approach for modeling RV data of resonant systems in which the system is assumed to reside in a particular MMR configuration called an “apsidal corotation resonance” (ACR). The ACR is the expected outcome of resonant capture under the influence of smooth convergent migration and eccentricity damping, and it has zero libration amplitude. Hadden & Payne (2020) used Bayesian model comparison to assess the evidence in RV data for the ACR model versus a conventional model, and they identified several systems in which the zero- A_{lib} ACR model is preferred. It is possible that such a model could be extended to include finite libration amplitude configurations as well.

In the case where the conventional approach is to be adopted with no modifications, it is important to be aware of the existence of the bias, particularly when making broader statements on the basis of the inferred libration amplitude. One could explore tests such as varying the size of the dataset going into the fit and seeing how the resulting libration amplitude distributions differ. This could help determine whether or not the distribution is converging. It is also generally appropriate to assume that the true libration amplitude is more closely approximated by values towards the low end of the inferred distribution, as opposed to the mean or median (e.g. Figure 5).

6. CONCLUSION

Exoplanetary systems containing mean-motion resonances offer valuable tests of planet migration and protoplanetary disk properties. However, a key ingredient in an accurate characterization of a resonance is a reliable estimate of the libration amplitude, or the range of oscillations of the critical angle, which indicate how “deep” in

resonance a system actually is. Motivated by prior work on the GJ 876 system by Millholland et al. (2018), here we showed that the reliability of libration amplitude inferences from observations of resonant systems depends sensitively on the data quality and the degree of measurement noise. Specifically, when using conventionally-adopted uninformative priors, progressively larger measurement noise causes the libration amplitude distribution inferred from the posterior distribution of model parameters to be strongly biased towards larger values.

We showed this using two methods of scrutiny of a representative resonant system, HD 128311, which contains two eccentric super-Jupiter-sized planets in a 2:1 MMR with orbital periods equal to ~ 460 days and ~ 910 days (Rein 2015). The first approach involved a simulated broadening of the posterior distribution of system parameters, mimicking the effects of increasing measurement noise. The second approach involved performing dynamical fits of synthetic data with various levels of noise. In both approaches, the resulting libration amplitude distributions were found to systematically shift to larger values with more noise. Moreover, the synthetic data experiments revealed that even low levels of measurement noise result in inferred libration amplitude distributions that are systematically larger than the “true” value.

We highlighted some strategies for mitigating the bias. Specifically, we showed how the simple inclusion of a Gaussian-like penalty term in the prior can avoid the

posterior distribution being weighted to large libration amplitudes. Other modifications to the prior are also possible. If the conventional approach is still to be adopted with no modifications, one can examine the extent of the inevitable bias by observing the width of the libration amplitude distribution. (A broader distribution generally indicates a stronger bias.) Another approach is to vary the size of the dataset that is going into the parameter inference and observe whether the libration amplitude distribution is converging or varying strongly with the size of the dataset. In general, an awareness of the existence of the bias will strengthen our ability to characterize resonant systems and to decipher their formation histories.

7. ACKNOWLEDGEMENTS

We are very grateful to the referee, Sam Hadden, for his insightful comments and valuable suggestions, particularly with regard to the content in Sections 5.1 and 5.2. We are also grateful to Hanno Rein for sharing the posterior samples of HD 128311 from Rein (2015). We also thank Eric Ford, Dan Foreman-Mackey, and Greg Laughlin for helpful conversations, as well as Neta Bahcall for her help in facilitating this work through Princeton’s Junior Project requirement. S.C.M. was supported by NASA through the NASA Hubble Fellowship grant #HST-HF2-51465 awarded by the Space Telescope Science Institute, which is operated by the Association of Universities for Research in Astronomy, Inc., for NASA, under contract NAS5-26555.

REFERENCES

- Adams, F. C., Laughlin, G., & Bloch, A. M. 2008, *ApJ*, 683, 1117, doi: [10.1086/589986](https://doi.org/10.1086/589986)
- Batygin, K., Deck, K. M., & Holman, M. J. 2015, *AJ*, 149, 167, doi: [10.1088/0004-6256/149/5/167](https://doi.org/10.1088/0004-6256/149/5/167)
- Batygin, K., & Morbidelli, A. 2013, *A&A*, 556, A28, doi: [10.1051/0004-6361/201220907](https://doi.org/10.1051/0004-6361/201220907)
- Butler, R. P., Marcy, G. W., Vogt, S. S., et al. 2003, *ApJ*, 582, 455, doi: [10.1086/344570](https://doi.org/10.1086/344570)
- Dawson, R. I., Huang, C. X., Brahm, R., et al. 2021, *AJ*, 161, 161, doi: [10.3847/1538-3881/abd8d0](https://doi.org/10.3847/1538-3881/abd8d0)
- Delisle, J. B. 2017, *A&A*, 605, A96, doi: [10.1051/0004-6361/201730857](https://doi.org/10.1051/0004-6361/201730857)
- Dempsey, A. M., & Nelson, B. E. 2018, *ApJ*, 867, 75, doi: [10.3847/1538-4357/aae36c](https://doi.org/10.3847/1538-4357/aae36c)
- Fabrycky, D. C., Lissauer, J. J., Ragozzine, D., et al. 2014, *ApJ*, 790, 146, doi: [10.1088/0004-637X/790/2/146](https://doi.org/10.1088/0004-637X/790/2/146)
- Foreman-Mackey, D., Hogg, D. W., Lang, D., & Goodman, J. 2013, *PASP*, 125, 306, doi: [10.1086/670067](https://doi.org/10.1086/670067)
- Gillon, M., Triaud, A. H. M. J., Demory, B.-O., et al. 2017, *Nature*, 542, 456, doi: [10.1038/nature21360](https://doi.org/10.1038/nature21360)
- Goldreich, P., & Schlichting, H. E. 2014, *AJ*, 147, 32, doi: [10.1088/0004-6256/147/2/32](https://doi.org/10.1088/0004-6256/147/2/32)
- Goldreich, P., & Tremaine, S. 1980, *ApJ*, 241, 425, doi: [10.1086/158356](https://doi.org/10.1086/158356)
- Goodman, J., & Weare, J. 2010, *Communications in Applied Mathematics and Computational Science*, 5, 65, doi: [10.2140/camcos.2010.5.65](https://doi.org/10.2140/camcos.2010.5.65)
- Hadden, S., & Payne, M. J. 2020, *AJ*, 160, 106, doi: [10.3847/1538-3881/aba751](https://doi.org/10.3847/1538-3881/aba751)
- Henrard, J., & Lemaître, A. 1983, *Celestial Mechanics*, 30, 197, doi: [10.1007/BF01234306](https://doi.org/10.1007/BF01234306)
- Hogg, D. W., Myers, A. D., & Bovy, J. 2010, *ApJ*, 725, 2166, doi: [10.1088/0004-637X/725/2/2166](https://doi.org/10.1088/0004-637X/725/2/2166)
- Hühn, L. A., Pichierri, G., Bitsch, B., & Batygin, K. 2021, *A&A*, 656, A115, doi: [10.1051/0004-6361/202142176](https://doi.org/10.1051/0004-6361/202142176)

- Laughlin, G., Butler, R. P., Fischer, D. A., et al. 2005, *ApJ*, 622, 1182, doi: [10.1086/424686](https://doi.org/10.1086/424686)
- Lucy, L. B., & Sweeney, M. A. 1971, *AJ*, 76, 544, doi: [10.1086/111159](https://doi.org/10.1086/111159)
- Marcy, G. W., Butler, R. P., Fischer, D., et al. 2001, *ApJ*, 556, 296, doi: [10.1086/321552](https://doi.org/10.1086/321552)
- McArthur, B. E., Benedict, G. F., Henry, G. W., et al. 2014, *ApJ*, 795, 41, doi: [10.1088/0004-637X/795/1/41](https://doi.org/10.1088/0004-637X/795/1/41)
- Millholland, S., & Laughlin, G. 2019, *Nature Astronomy*, 3, 424, doi: [10.1038/s41550-019-0701-7](https://doi.org/10.1038/s41550-019-0701-7)
- Millholland, S., Laughlin, G., Teske, J., et al. 2018, *AJ*, 155, 106, doi: [10.3847/1538-3881/aaa894](https://doi.org/10.3847/1538-3881/aaa894)
- Mills, S. M., Fabrycky, D. C., Migaszewski, C., et al. 2016, *Nature*, 533, 509, doi: [10.1038/nature17445](https://doi.org/10.1038/nature17445)
- Murray, C. D., & Dermott, S. F. 1999, *Solar system dynamics*
- Nelson, B. E., Robertson, P. M., Payne, M. J., et al. 2016, *MNRAS*, 455, 2484, doi: [10.1093/mnras/stv2367](https://doi.org/10.1093/mnras/stv2367)
- Nesvorný, D., Chrenko, O., & Flock, M. 2022, *ApJ*, 925, 38, doi: [10.3847/1538-4357/ac36cd](https://doi.org/10.3847/1538-4357/ac36cd)
- Nesvorný, D., & Vokrouhlický, D. 2016, *ApJ*, 823, 72, doi: [10.3847/0004-637X/823/2/72](https://doi.org/10.3847/0004-637X/823/2/72)
- Peale, S. J. 1976, *ARA&A*, 14, 215, doi: [10.1146/annurev.aa.14.090176.001243](https://doi.org/10.1146/annurev.aa.14.090176.001243)
- Rein, H. 2015, *MNRAS*, 448, L58, doi: [10.1093/mnrasl/slu202](https://doi.org/10.1093/mnrasl/slu202)
- Rein, H., & Liu, S. F. 2012, *A&A*, 537, A128, doi: [10.1051/0004-6361/201118085](https://doi.org/10.1051/0004-6361/201118085)
- Rein, H., & Papaloizou, J. C. B. 2009, *A&A*, 497, 595, doi: [10.1051/0004-6361/200811330](https://doi.org/10.1051/0004-6361/200811330)
- Rein, H., & Spiegel, D. S. 2015, *MNRAS*, 446, 1424, doi: [10.1093/mnras/stu2164](https://doi.org/10.1093/mnras/stu2164)
- Rivera, E. J., Laughlin, G., Butler, R. P., et al. 2010, *ApJ*, 719, 890, doi: [10.1088/0004-637X/719/1/890](https://doi.org/10.1088/0004-637X/719/1/890)
- Rivera, E. J., Lissauer, J. J., Butler, R. P., et al. 2005, *ApJ*, 634, 625, doi: [10.1086/491669](https://doi.org/10.1086/491669)
- Shen, Y., & Turner, E. L. 2008, *ApJ*, 685, 553, doi: [10.1086/590548](https://doi.org/10.1086/590548)
- Silburt, A., & Rein, H. 2017, *MNRAS*, 469, 4613, doi: [10.1093/mnras/stx1193](https://doi.org/10.1093/mnras/stx1193)
- Terquem, C., & Papaloizou, J. C. B. 2007, *ApJ*, 654, 1110, doi: [10.1086/509497](https://doi.org/10.1086/509497)
- Vogt, S. S., Butler, R. P., Marcy, G. W., et al. 2005, *ApJ*, 632, 638, doi: [10.1086/432901](https://doi.org/10.1086/432901)
- Wisdom, J. 2015, *AJ*, 150, 127, doi: [10.1088/0004-6256/150/4/127](https://doi.org/10.1088/0004-6256/150/4/127)
- Wisdom, J., & Holman, M. 1991, *AJ*, 102, 1528, doi: [10.1086/115978](https://doi.org/10.1086/115978)
- Wright, J. T., Veras, D., Ford, E. B., et al. 2011, *ApJ*, 730, 93, doi: [10.1088/0004-637X/730/2/93](https://doi.org/10.1088/0004-637X/730/2/93)